LMM and LMN Auger spectra of Nb, Mo, Pd and Ag: an investigation by X-ray excited Auger

electron spectroscopy

LMM and LMN Auger spectra of Nb, Mo, Pd and Ag: an investigation by x-ray-excited Auger electron spectroscopy

R Landers, P A P Nascente, S G C de Castro and G G Kleiman

Departmento de Física Aplicada, Instituto de Física 'Gleb Wataghin', Universidade Estadual de Campinas, Caixa Postal 6165, 13081-Campinas, SP, Brazil

Abstract. We present high-resolution measurements of several of the LMM and LMN Auger spectra of Nb, Mo, Pd and Ag excited by bremsstrahlung. Because of their high energy (2.0–3.5 keV), these spectra have not been reported in the literature. Assignments of the peaks are made based upon energy and intensity considerations.

1. Introduction

Considerable interest in high-resolution Auger spectroscopy of transition and noble metals and their alloys has arisen because of the possibility of extracting new information regarding electronic structure [1–5]. Auger transitions whose final states involve only core levels (which we denote as ijk spectra) are especially interesting in this regard since current theoretical interpretations of lineshapes [6–8] and energies [9–11] in these materials assume, in general, that the final core holes are either atomic or quasi-atomic. Among topics of interest are comparisons of the results of atomic calculations with spectra measured by x-ray-excited Auger electron spectroscopy (XAES) [12–15], investigations of the Auger parameter [12, 15–20] and applications of Auger kinetic energy shifts in alloys to extracting information regarding electronic structure changes [3, 21–23].

Reports of such high-resolution spectra in the literature are few, however. Usually, such spectra are either broad, partially as a result of the superposition of contributions from various terms, as in the case of the $L_{2,3}M_{2,3}M_{2,3}$ spectra of the 3d series [12] and the $N_{6,7}O_{4,5}O_{4,5}$ spectra of Tl, Pb and Bi [13], or they are weak in intensity and, necessarily, of very high kinetic energies, as in the case of the $L_{2,3}M_{4,5}M_{4,5}$ spectra of the 4d series [14, 15]. For these reasons, it is not common to study Auger transitions involving only core levels experimentally.

In the 4d series, in particular, the most commonly measured spectra correspond to the $M_{4,5}N_{4,5}N_{4,5}$ Auger transitions. Since the final-state holes of these transitions reside in the valence band, however, the lineshapes vary dramatically with different chemical environments. This dependence and the fact that these spectra are generally rather broad reduce their usefulness in many cases.

For these reasons, it is desirable to measure ijk transitions of the 4d metals. The LMM and LMN Auger transitions are suitable candidates, despite their weak intensities and high kinetic energies (i.e. from 2.0 to 3.5 keV). Most of them are
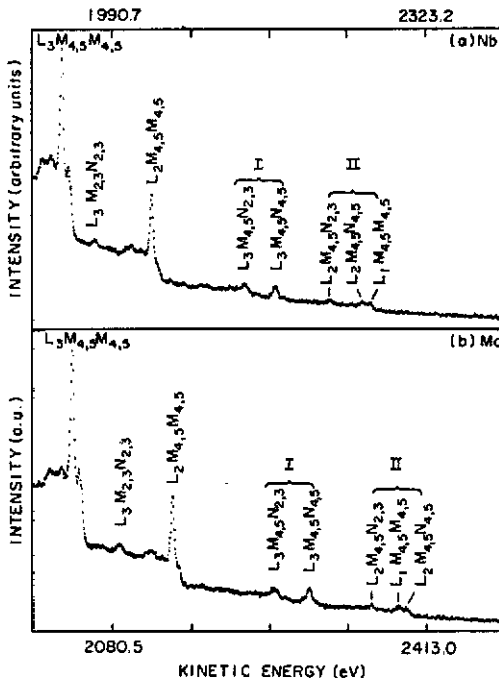
Figure 1. (a) Long scan from 1907.6 to 2406.3 eV of the Nb spectra. The assignments described in the text are indicated. Regions I and II correspond to detailed spectra in figures 3(a) and 5(a), respectively. (b) Long scan from 1997.4 to 2496.1 eV of the Mo spectra. Regions I and II correspond to figures 3(b) and 5(b), respectively.

relatively narrow and the various contributions are usually well separated in energy, thereby facilitating theoretical interpretation.

In recent work [14, 15, 19, 20], we reported measurements of the $L_{2,3}M_{4,5}M_{4,5}$ Auger spectra of Nb, Mo, Ru, Pd, Ag, In, Sn and Sb. A considerable amount of electronic structure information can be extracted from these measurements. In particular, measurement of the Auger parameter of these metals for these transitions clarifies the valence electron screening mechanisms of the core holes [15, 19, 20]. In addition, study of the evolution of the experimental lineshapes between open- and closed-valence-shell metals may have important consequences for theoretical investigations.

We can expect to be able to obtain similar information from measurements of the other high-energy LMM and LMN spectra. An interesting point is the possibility of observing and comparing transitions whose final states have either two core holes or a core hole and a valence hole (i.e. the LMM and LMN transitions, respectively). From such a comparison, for example, insight into the different screening mechanisms can be expected to be inferred.

Here, we present LMN and LMM Auger spectra excited by bremsstrahlung [24, 25] for metallic Nb, Mo, Pd and Ag. The experimental features are tentatively identified using both energy predictions from the x-ray tables [26] and intensity estimates [27]. To our knowledge, this is the first time that such data have been reported.

In the next section we present the experimental details on the sample preparation and analyser calibration. In section 3, we present the XAES results in the form of
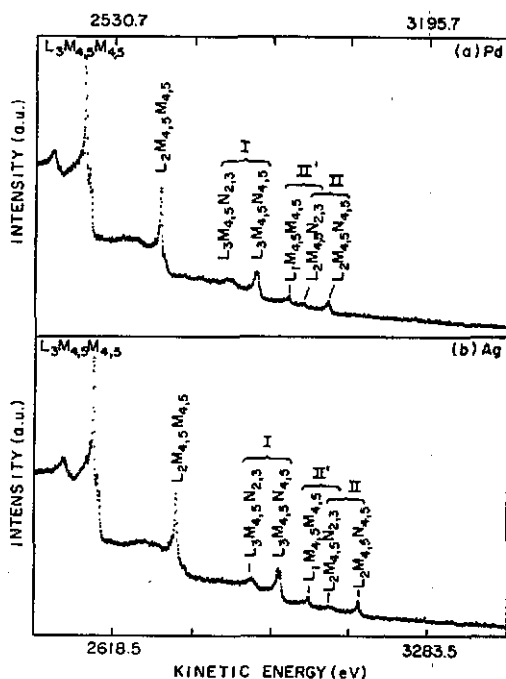
Figure 2. (a) Long scan from 2364.4 to 3362.0 eV of the Pd spectra. Regions I and II correspond to figures 4(a) and 6(a), respectively. Region II' is exhibited in figure 7(a). (b) Long scan from 2452.2 to 3449.7 eV of the Ag spectra. Regions I and II correspond to figures 4(b) and 6(b), respectively. Region II' is exhibited in figure 7(b).

tables and as raw experimental spectra and briefly discuss the identification of the various features. The conclusions are presented in section 4.

2. Experimental procedure

Polycrystalline samples of Nb, Mo, Pd and Ag were cold rolled (except for Mo) and polished using standard metallurgical techniques. The resulting four metallic foils were mounted on a mobile carousel. Sample cleaning was performed *in situ* by several cycles of Ar ion bombardment and annealing until only traces of O, C and S could be observed by x-ray photoemission spectroscopy (XPS) [28].

The XAES and XPS measurements were made using an ion-pumped system (base pressure of $(2-5) \times 10^{-10}$ Torr) with a Vacuum Science Workshop HA 100 hemispherical (100 mm mean radius) analyser. Both Al and Mg Kα excitations ($h\nu = 1486.6$ eV and 1253.6 eV, respectively) were employed and the high-kinetic-energy (above 1500 eV) Auger spectra were excited by bremsstrahlung radiation [24, 25]. Both Al and Mg anodes were operated with 15.0 mA emission current at 12.0 kV voltage.

We should point out that the intensities of these lines are very small because bremsstrahlung is several orders of magnitude less intense than the characteristic Kα radiation. In order to reduce the data collection time, we were obliged to use high transmission, i.e. a pass energy of 90.0 eV, which produces an FWHM for the Au $4f_{7/2}$ line of 1.5 eV. This resolution did not prove limiting since the Auger lines are

Table 1. Experimental (E) and x-ray-table-derived (T) kinetic energies [29] plus McGuire's [27] transition rates multiplied by $(2J+1)/2\pi$, where $2J+1$ is the multiplicity of the initial hole.

Transition		Kinetic energy (eV)				McGuire's transition rate $(10^{-4}\ \mathrm{au}^{-1})$	
		Nb	Mo	Pd	Ag	Zr	Ag
$L_3M_{4,5}M_{4,5}$	(E)	1938.3	2038.8	2469.2	2576.7	154.56	176.39
	(T)	1961.4	2063.0	2499.7	2611.7		
$L_2M_{4,5}M_{4,5}$	(E)	2032.8	2143.5	2626.0	2750.3	77.46	88.04
	(T)	2055.4	2168.0	2656.6	2784.3		
$L_1M_{4,5}M_{4,5}$	(E)	2264.5	2384.2	2899.6	3032.0	32.92	38.60
	(T)	2288.8	2408.6	2930.0	3066.4		
$L_3M_3N_{2,3}$	(E)	1973.3	2088.0			11.94	15.64
	(T)	1976.7	2092.5	2591.2	2721.2		
$L_2M_3N_{2,3}$	(E)					5.98	7.82
	(T)	2070.6	2197.5	2748.2	2893.8		
$L_3M_{4,5}N_{2,3}$	(E)	2129.4	2251.7	2775.5[a]	2909.2[a]	14.20	14.66
	(T)	2134.8	2257.0	2785.1	2923.3		
$L_3M_{4,5}N_{4,5}$	(E)	2163.1	2288.8	2827.3	2966.2	4.94	44.06
	(T)	2163.7	2289.4	2834.9	2977.6		
$L_2M_{4,5}N_{2,3}$	(E)	2222.0	2354.9	2930.0[a]	3080.2[a]	7.10	7.34
	(T)	2228.7	2362.0	2942.1	3095.9		
$L_2M_{4,5}N_{4,5}$	(E)	2255.8	2391.6	2983.8	3138.7	2.46	21.98
	(T)	2257.7	2394.4	2991.9	3150.2		

[a] Very broad lines.

Table 2. Auger parameter ξ_{ijk} for the indicated ijk transitions. (ξ_{ijk} is the difference between the theoretical and experimental Auger kinetic energies in table 1.)

	ξ_{ijk}			
	Nb	Mo	Pd	Ag
$L_3M_{4,5}M_{4,5}$	23.1	24.2	30.5	35.0
$L_2M_{4,5}M_{4,5}$	22.6	24.5	30.6	34.0
$L_1M_{4,5}M_{4,5}$	24.3	24.4	30.4	34.4
$L_3M_3N_{2,3}$	3.4	4.5		
$L_3M_{4,5}N_{2,3}$	5.4	5.3	9.6[a]	14.1[a]
$L_3M_{4,5}N_{4,5}$	0.6	0.6	7.6	11.4
$L_2M_{4,5}N_{2,3}$	6.7	7.1	12.1[a]	15.7[a]
$L_2M_{4,5}N_{4,5}$	1.9	2.8	8.1	11.5

[a] Very broad lines.

relatively broad; we verified this by measuring the higher-intensity $L_3M_{4,5}M_{4,5}$ spectra with better-resolution fixed analyser transmission (FAT) modes also and observed no
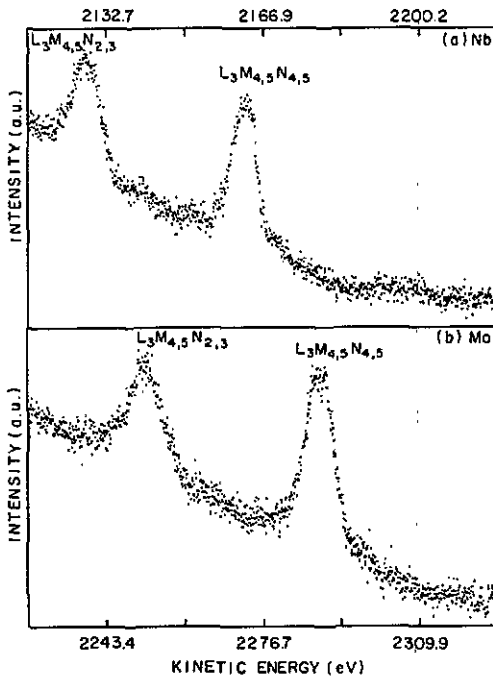
Figure 3. (a) Detailed spectra of the $L_3M_{4,5}N_{2,3}$ and $L_3M_{4,5}N_{4,5}$ transitions for Nb. (b) Analogous spectra for Mo.

extra structure. Measurement of the high-resolution spectra took from 12 to 16 h.

A careful calibration of the spectrometer was carried out by precisely biasing a clean Au foil in order to shift the kinetic energy of the $4f_{7/2}$ electrons (binding energy, 84.0 eV) to the energy range of interest [15]. The XAES spectra were referenced to the Fermi level of the spectrometer.

3. Results

Figures 1(a) and 1(b) respectively, display long scans of Nb and Mo through the energy regions in which we find the LMM and LMN Auger spectra of interest (1907.6–2406.3 eV for Nb and 1997.4–2496.1 eV for Mo). Corresponding scans for Pd (2364.4–3362.0 eV) and Ag (2452.2–3449.7 eV) appear in figures 2(a) and 2(b), respectively. Identifications of the features indicated in figures 1 and 2 were made based upon both energy predictions from Bearden's [26] x-ray tables and intensity estimates from McGuire's [27] tables.

The regions indicated as I and II in figure 1(a) correspond to detailed scans in figures 3(a) and 5(a), respectively; regions I and II in figure 1(b) correspond to figures 3(b) and 5(b), respectively. Regions I and II in figure 2(a) represent figures 4(a) and 6(a), respectively, while those in figure 2(b) represent figures 4(b) and 6(b), respectively. The region II' overlapping region II in figure 2 corresponds to figure 7.

Table 1 presents the measured kinetic energies of the Auger peaks shown in figures 1–7, as well as the respective predicted energies derived from the x-ray tables [26, 29]. The measured kinetic energies were taken from the most intense feature of
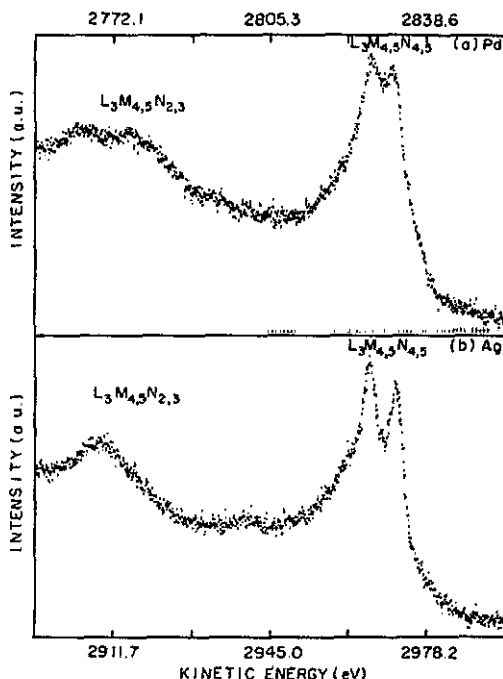
Figure 4. (a) Detailed spectra of the $L_3M_{4,5}N_{2,3}$ and $L_3M_{4,5}N_{4,5}$ transitions for Pd. The $L_3M_{4,5}N_{2,3}$ spectrum is very broad, impeding determination of the peak energy. Only estimates of this energy are given in table 1. (b) Detailed spectra of the $L_3M_{4,5}N_{2,3}$ and $L_3M_{4,5}N_{4,5}$ transitions for Ag. Because of the breadth of the $L_3M_{4,5}N_{2,3}$ peak, only estimates of its energy are given in table 1.

each spectrum. The energies of those features outside regions I, II and II' in figures 1 and 2 were taken from the long scans; otherwise, the energies are obtained from the detailed spectra in figures 3–7. Table 1 also presents McGuire's [27] transition rates (in 10^{-4} au^{-1}) for Zr and Ag weighted by the multiplicity of the initial core hole [12]; the transitions indicated correspond to those of strongest intensity. Derived Auger parameters [29–31] are displayed in table 2.

Of the spectra shown in figures 1 and 2, we discuss the $L_{2,3}M_{4,5}M_{4,5}$ spectra in detail elsewhere [14, 15] and reserve the well defined structure below the $L_3M_{4,5}M_{4,5}$ spectra for a future publication. One peak in figure 1 which does not appear in the detailed spectra lies between $L_3M_{4,5}M_{4,5}$ and $L_2M_{4,5}M_{4,5}$ and we tentatively identify it as $L_3M_3N_{2,3}$ in the figures. This assignment is based on the agreement between measured and predicted energies, as well as on the consistency of the measured intensity with that predicted and with that of other experimental features (e.g. $L_3M_{4,5}N_{2,3}$), as shown in table 1. An apparent problem with this assignment arises when we observe that the $L_3M_3N_{2,3}$ peak is predicted to have a similar intensity for Ag, but that it fails to appear in either the Pd or the Ag long scans anywhere near the predicted energy.

This difference between the Nb–Mo and Pd–Ag spectra may be related to dipolar fluctuations of the $4p_{1/2}$ and $4p_{3/2}$ core holes in the atoms near Xe in the periodic table, which invalidate the one-particle description of these levels and cause relaxation shifts, spectral redistributions and shape changes, and large widths of the corresponding 4p XPS lines [4, 32, 33]. The effect of these fluctuations depends on the degree to
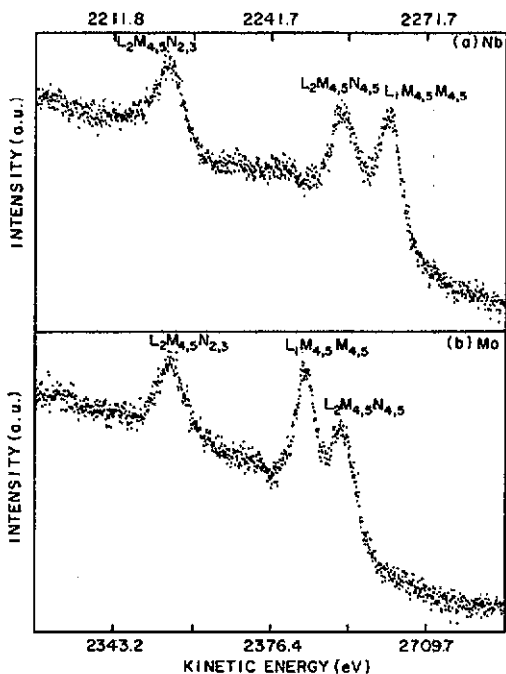
Figure 5. (a) Detailed spectra of the $L_2M_{4,5}N_{2,3}$ and $L_2M_{4,5}N_{4,5}$ transitions for Nb. Also displayed is the $L_1M_{4,5}M_{4,5}$ spectrum. (b) Analogous spectra for Mo.

which the 4p hole levels are degenerate with the $[4d^2]\epsilon f$ double-ionization continuum (i.e. two 4d holes and a continuum state electron). Since the measured 4p linewidths [30, 34] in Ag and Pd are much larger than in Nb and Mo, one expects this effect to be much larger in the former than in the latter metals, which could explain our failure to observe the putative $L_3M_3N_{2,3}$ transition in Pd and Ag.

It should be pointed out that another peak of comparable intensity just below the $L_2M_{4,5}M_{4,5}$ line in the Nb and Mo long scans does not appear to correspond to any predicted Auger transition of significant intensity; this peak, too, does not appear in figure 2. The analogous behaviour of this unidentified peak raises questions concerning our assignment of $L_3M_3N_{2,3}$.

Comparison of figures 3 and 4 shows that the $L_3M_{4,5}N_{2,3}$ Auger peaks are sharper for Nb and Mo than for Pd and Ag. The $L_2M_{4,5}N_{2,3}$ peaks shown in figures 5 and 6 seem to have the same behaviour. This behaviour would seem to agree with our discussion above of the $L_3M_3N_{2,3}$ transition. It is interesting to note, however, that, in contrast with the $L_3M_3N_{2,3}$ transition, the $L_{2,3}M_{4,5}N_{2,3}$ spectra are observable in all four metals, even though the predicted transition rates in table 1 are comparable for the $L_3M_{4,5}N_{2,3}$ spectra and smaller for the $L_2M_{4,5}N_{2,3}$ spectra.

The $L_3M_{4,5}N_{4,5}$ peaks displayed in figure 4 present a clear double structure for Pd and Ag, while for Nb and Mo (figure 3) this structure is not observed. Double structures are also seen for the corresponding $L_2M_{4,5}N_{4,5}$ lines in figure 6, although not so prominently (especially for Pd). Figure 5 shows the $L_1M_{4,5}M_{4,5}$ Auger peaks for Nb and Mo. The corresponding peaks for Pd and Ag are displayed in figure 7.

An interesting point is that the $L_3M_{4,5}N_{4,5}$ and $L_2M_{4,5}N_{4,5}$ intensities (figures 3 and 5) for Nb and Mo compared with the $L_{2,3}M_{4,5}N_{2,3}$ intensities do not reflect the
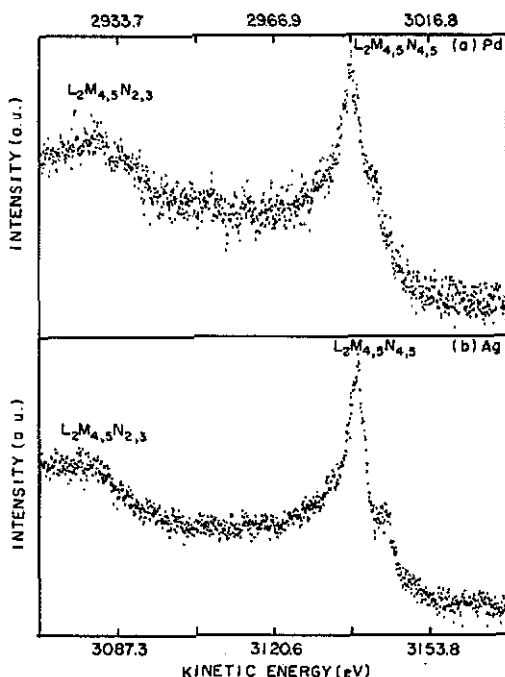
Figure 6. (a) Detailed spectra of the $L_2M_{4,5}N_{2,3}$ and $L_2M_{4,5}N_{4,5}$ transitions for Pd. Because of the breadth of the $L_2M_{4,5}N_{2,3}$ peak, only estimates of its energy are given in table 1. (b) Analogous spectra for Ag.

relation given by McGuire [27] for Zr. On the other hand, his transition rates for the $L_{2,3}M_{4,5}N_{4,5}$ and $L_{2,3}M_{4,5}N_{2,3}$ intensities of Ag seem to describe adequately the experimental spectra shown in figures 4 and 6.

In order to verify our assignments, we calculated the Auger parameters presented in table 2 [29–31]. These quantities represent the effective Coulomb interaction between the final-state holes. From general arguments [16], we expect these quantities to depend upon the final state only, and to be larger for both holes with the same principal quantum number than for those in different atomic shells. This expectation is borne out by the close agreement between all the transitions with $M_{4,5}M_{4,5}$ final hole states and by the fair agreement between those with $M_{4,5}N_{2,3}$ and $M_{4,5}N_{4,5}$ final hole states. The decrease in the Auger parameter magnitudes as we proceed from $M_{4,5}M_{4,5}$ to $M_{4,5}N_{2,3}$ to $M_{4,5}N_{4,5}$ final hole states also supports the assignment from considerations of the annular spatial regions in which the holes reside.

4. Conclusions

In this paper, we demonstrate, for the first time, the possibility of making high-resolution measurements of the high-kinetic-energy (from 1900 to 3450 eV) LMM and LMN XAES spectra of Nb, Mo, Pd and Ag. The resulting spectra, although weak in intensity, as manifested in figures 1 and 2, are, in general, at least as narrow and well defined as those of the 3d [12] and 5d [13] metals previously studied.

The Auger features were tentatively assigned using both energy predictions from x-ray tables and intensity estimates. Verification of the assignments rests upon the
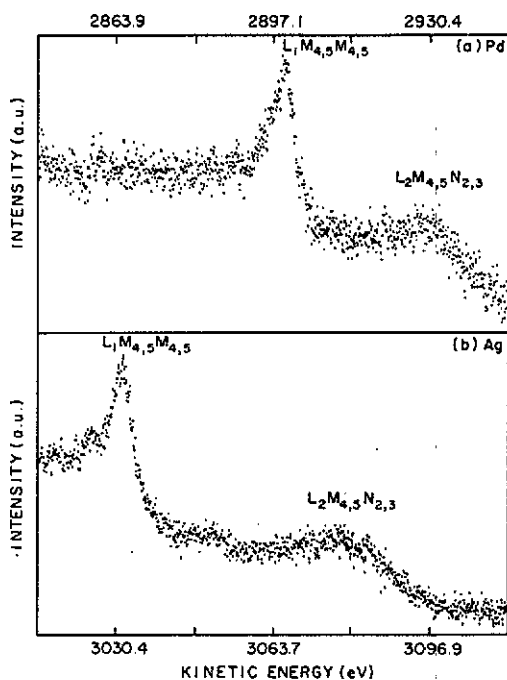
Figure 7. (a) The $L_1M_{4,5}M_{4,5}$ and $L_2M_{4,5}N_{2,3}$ spectra for Pd. Note the breadth of the $L_2M_{4,5}N_{2,3}$ peak. (b) Analogous spectra for Ag.

agreement between the measured and predicted features of the spectra, as well as upon the experimental systematics of the Auger parameter, or effective final-state hole–hole Coulomb interaction [16]. Spectral features assigned the same final two-hole state exhibit Auger parameters which agree in magnitude, as we expect from general considerations [16]. In addition, assigned final states whose holes reside in different shells have smaller Auger parameters than those in the same shell, which, again, agrees with expectations [16].

Both the $L_3M_{4,5}N_{2,3}$ and the $L_2M_{4,5}N_{2,3}$ Auger peaks are sharper for Nb and Mo than for Pd and Ag. The $L_3M_{4,5}N_{4,5}$ peaks of Pd and Ag present a double structure, in contrast with the single feature observed for Nb and Mo. The same behaviour seems to occur for the respective $L_2M_{4,5}N_{4,5}$ lines.

Theoretical estimates [27] for Ag, a closed-valence-shell metal, agree with experimental intensities, whereas that for Zr, an open-shell metal, do not. It would seem that the availability of systematic high-resolution spectra, such as we present here, is important for improving the theoretical understanding of open-shell systems.

Acknowledgments

References

[1]   Fuggle J C 1981 *Electron Spectroscopy* ed C R Brundle and A D Baker (London: Academic) p 85
[2]   Madden H H 1981 *J. Vac. Sci. Technol.* **18** 677
[3]   Kleiman G G 1982 *Appl. Surf. Sci.* **11–12** 730
[4]   Weightman P 1982 *Rep. Prog. Phys.* **45** 753
[5]   Houston J E and Rye R R 1983 *Comment. Solid State Phys.* **10** 233
[6]   Cini M 1976 *Solid State Commun.* **20** 605
[7]   Sawatzky G A 1977 *Phys. Rev. Lett.* **39** 504
[8]   McGuire E J 1975 *Atomic Inner-Shell Processes* ed B Crasemann (London: Academic) p 293
[9]   Lang N D and Williams A R 1977 *Phys. Rev.* B **16** 2408
[10] Williams A R and Lang N D 1978 *Phys. Rev. Lett.* **40** 954
[11] Johansson B and Mårtensson N 1980 *Phys. Rev.* B **21** 4427
[12] Antonides E, Janse E C and Sawatzky G A 1977 *Phys. Rev.* B **15** 1669
[13] McGilp J F, Weightman P and McGuire E J 1977 *J. Phys. C: Solid State Phys.* **10** 3445
[14] Kleiman G G, Landers R, Nascente P A P and de Castro S G C 1992 *Phys. Rev.* B at press
[15] Kleiman G G, Landers R, Nascente P A P and de Castro S G C 1992 *Phys. Rev.* B at press
[16] Lang N D and Williams A R 1979 *Phys. Rev.* B **20** 1369
[17] Kleiman G G, de Castro S G C, Rogers J D and Sundaram V S 1982 *Solid State Commun.* **43** 257
[18] Rogers J D, Sundaram V S, Kleiman G G, de Castro S G C, Douglas R A and Peterlevitz A C 1982 *J. Phys. F: Met. Phys.* **12** 2097
[19] Kleiman G G, Landers R, de Castro S G C and Nascente P A P 1991 *Phys. Rev.* B **44** 3383
[20] Kleiman G G, Landers R, de Castro S G C and Nascente P A P 1992 *J. Vac. Sci. Technol.* A **10** at press
[21] Nascente P A P, de Castro S G C, Landers R and Kleiman G G 1991 *Phys. Rev.* B **43** 4659
[22] Thomas T D and Weightman P 1986 *Phys. Rev.* B **33** 5406
[23] Kleiman G G, Landers R, de Castro S G C and Rogers J D 1991 *Phys. Rev.* B **44** 8529
[24] Wagner C D and Taylor J A 1980 *J. Electron Spectrosc. Relat. Phenom.* **20** 83
[25] Sundaram V S, Rogers J D and Landers R 1981 *J. Vac. Sci. Technol.* **19** 117
[26] Beardean J A 1967 *Rev. Mod. Phys.* **39** 78
[27] McGuire E J 1971 *Sandia Laboratory Report* SC-RR-710075
[28] Musket R G, McLean W, Colmenares C A, Makowiecki D M and Siekhaus W J 1982 *Appl. Surf. Sci.* **10** 143
[29] The predicted Auger energies were calculated according to the prescription in [30], which uses weighted averages of the final hole energies. The L_3 binding energy was derived by combining the M_5 binding energy from [31] with the L_3 α_1 x-ray energy [26]. All other binding energies were derived by adding appropriate x-ray energies [26] to this L_3 value
[30] Mårtensson N and Nyholm R 1981 *Phys. Rev.* B **24** 7121
[31] Wagner C D, Riggs W M, Davis L E and Moulder J F 1979 *Handbook of X-ray Photoelectron Spectroscopy* ed G E Muilenberg (Eden Prairie, MN: Perkin–Elmer)
[32] Wendin G and Ohno M 1976 *Phys. Scr.* **14** 148
[33] Wendin G 1979 *Int. J. Quantum Chem.* **13** 659
[34] Fuggle J C and Alvarado S F 1980 *Phys. Rev.* B **22** 1615